High Gain 30 GHz Multi-Band Multi-Faceted Miniature Antenna for 5G and Cancer Detection

Maria Moussa[1], Mervat A. Madi[1], Karim Y. Kabalan[1], Zeeshan Ahmed[2], and Max J Ammann[2]

[1]ECE Department, American University of Beirut, Beirut, Lebanon
[2]TU Dublin, Antenna and High Frequency Research Center, Dublin, Ireland

***Abstract*—This paper proposes a microstrip antenna array for fifth generation mobile communication systems. The antenna is triangle-fractal-shaped printed on an aluminum oxide ceramic substrate. It has equal sides of 22 mm length and a 29 mm base. Aiming at a 30 GHz frequency and a high gain operation, a multi-band antenna is simulated. A good agreement with acceptable frequency shift between simulations and measurements with a measured gain above 8 dB is achieved. Multiple three-dimensional antenna designs are discussed for broad-band operation necessary for 5G operation.**

***Index Terms*—5G, antenna array, triangular patch, millimeter wave frequencies, gain, three-dimensional antennas.**

I. Introduction

Fifth generation networks present the future most demanded technology in the next major phase of mobile telecommunications thanks to their many advanced features overpassing the preceding technologies, [1]. Some of these features are good throughput, high bit rate, larger coverage range, better energy consumption as well as multiple concurrent paths which makes it able to serve billions of connected devices. As number of online users has increased exponentialy, 4G networks have reached the limit at a time when users want even more data for their devices as stated by the authors of [2]. 5G is supposed to handle a thousand times more traffic than current networks. Since 5G wireless systems are highly efficient systems supporting high capacity, [3], their main challenge is the use of higher frequency bands that can provide higher data rates and wider spectrum. Millimeter waves occupy the frequency spectrum from 30 GHz to 300 GHz with some drawbacks such as high propagation losses. Thanks to the many advantages of microstrip antennas such as light weight, low cost and ease of fabrication, they present the best kind of antennas that could be used. Some of the requirements for such antennas, [4], are high gain and highly directional patterns as well as small size, [5], with a suitable impedance matching bandwidth. According to [6], to get high antenna gain in a desired direction while having low side lobe levels in undesired directions, a designer should use planar arrays that allow obtaining directive beams.

A very simple patch antenna is proposed in [7]; it operates at 38.14 GHz with a return loss of -31 dB. It has a compact size which makes it suitable for the next generation (5G) wireless communication devices. It is fed using a coaxial probe feed and the substrate used is a Taconic RF-60™ substrate with a dielectric constant of 6.15. However more sophisticated patch antennas could be designed to meet up with the requirements of the future 5G networks. In [8], a slotted patch antenna operational at two frequency bands 28 GHz and 38 GHz is proposed. It is used in highly demanded MIMO systems in 5G networks. Some measurement results are presented which proves its performance in the near-field as well as the far-field. A dual band MIMO antenna system is proposed in [9]; it consists of eight dual band antennas operating at 3.5 GHz and 4.9 GHz placed in a suitable orientation to form the MIMO system used for 5G mobile phone applications. An array composed of eight inverted-F antennas (IFA) is proposed in [10]; it operates at 3.5 GHz and it has a compact size because it uses a coupled feed and a shorting meander strip line.

Two elements and four elements linear triangular patch antenna arrays are presented in [11] and a comparison was made between rectangular and triangular antenna arrays of the same size. The feeding network of the two elements is formed of a 50 Ohms input impedance split into two 100 Ohms transmission lines. However, a quarter wave transformer is used to feed the four elements array. It is proven that a triangular antenna array has approximately the same performance of a rectangular antenna array in terms of reflection coefficient but a better suppression of side lobe level could be achieved using the triangular shape. Also in [12], an array of 2 x 2 triangular patches is designed. It operates at 5.5 GHz and it is designed on an FR4 substrate with a dielectric constant of 4.4. The feeding network is also designed using a quarter wave transformer. Simulated results agreed with the measurements with an S_{11} of approximately -32 dB and a VSWR less than 2 as well as a high directivity.

The authors of [13] designed a phased antenna array that consists of eight 28 GHz Vivaldi antenna elements. The simulations showed a reflection coefficient less than -10 dB, a good gain, high efficiency and 3D beam steering characteristics in the band of operation, hence it can be considered a good candidate for millimeter wave 5G communications. The authors of [14] proposed a compact 3D antenna for LTE, GSM and UMTS vehicular applications. Two identical antennas of this type are considered together to form a MIMO system. Thanks to the small size of the single radiating element, it can be considered as a good candidate

to be integrated under the shark-fin cover of a vehicle.

In addition to the other features, 5G mobile communications could achieve higher peak data rates and lower latency. The authors of [15] present a Vivaldi antenna operating in the S and L bands, that could be used for 5G communications, with a large bandwidth covering [1.4 – 3.8] GHz with a gain higher than 7 dB. A coplanar waveguide fed microstrip antenna is proposed in [16]; it covers the 28 GHz and the 39 GHz bands. A wide band slot antenna bent at right angles is proposed in [17]; it has large operating bandwidths and achieves high gains of 10.9 dBi at 28 GHz and 12.7 dBi at 39 GHz. An antenna array composed of four element microstrip slots is presented in [18]; it operates at 28 GHz with a gain of 9.5 dBi.

Four types of 24 GHz 3D antenna structures are presented in [19] and each type showed an improvement in the performance of the antenna. Two of the four types designed presented maximum current at their surface which allowed the insertion of the feed deeper in the antenna and therefore making the size of the antenna more compact. Also the sizes of the 3D antennas designed exhibited reduction compared to the planar antennas designed for the same application. The improved antenna parameters such as its compact size as well as the wider bandwidth offers many benefits to on chip applications.

In this paper a triangular micro strip patch antenna is simulated using an aluminum oxide ceramic substrate with a dielectric constant of 9.8 and a thickness of 0.254 mm. It is operational at 30 GHz with a reflection coefficient of -42 dB and a gain of 5.9 dB. In a way to increase the directivity and the gain of the antenna, the number of elements is increased, and consequently the gain obtained is 8.57 dB, 9.26 dB, 12.51 dB and 13.03 dB for the two-elements, three-elements, fractal design of three-elements forming nine elements and the same fractal design with a triangular-shaped ground plane, respectively. All of the designs are matched at around 30 GHz. A parametric study was done on the side length of the triangle, the width of the transmission lines forming the feeding network, the length and width of the inset feed and the length of the 50 Ohms transmission line feeder to get the best gain in each design with the lowest S_{11} possible at 30 GHz.

This paper is divided into six sections. Section II presents the simulated designs of all the planar two-dimensional micro strip patch antennas. The final planar triangular design with nine elements is fabricated and presented in section III. Section III also contains a comparison between the simulated and the measured results after fabrication. The three-dimensional designs are presented in section IV. Section V presents further potential applications for the fabricated antenna. Finally, the paper will be concluded in section VI.

II. Two-Dimensional Antenna Array Designs

A. Single Element Triangular Patch Antenna

First, a triangular shaped patch antenna as shown in Fig. 1 is designed to operate at 30 GHz. Eq. (1) is used to determine the side length of the equilateral triangle, [20], where c represents the velocity of electromagnetic waves in free space, ϵ_r is the dielectric constant of the substrate, a is the side length and fi s the resonant frequency. This equation relates the side length of the patch with its resonance frequency. The value is found to be 2.13 mm; however, this value is only considered as a start point. A parametric study has to be done on this dimension to find the best value for a good performance at 30 GHz.

$$f = \frac{2c}{3a\sqrt{\epsilon_r}} \tag{1}$$

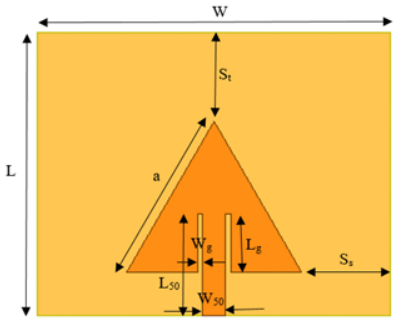

Fig. 1: Single patch antenna geometry.

A parametric study was done on the parameters such as the side length of the triangular patch, the spacing between the patch and the edges of the substrate from the top and at both sides, the width and length of the inset feed, etc.

TABLE I: Single patch antenna dimensions.

Parameters	Values (in mm)
L	3.19
W	3.96
a	1.96
S_t	1
S_s	1
W_g	0.06
L_g	0.66

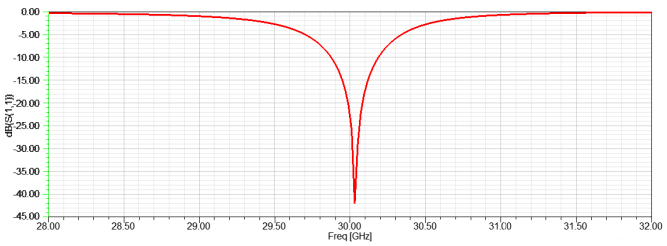

Fig. 2: S_{11} plot for the single patch antenna.

The 50 Ω transmission feed line has a fixed width, W_{50}, of 0.25 mm and a length, L_{50}, of 1.15 mm. The values chosen for these parameters are presented in table I. Matching is very

good at 30 GHz since the reflection coefficient is far below -10 dB, as shown in the S_{11} plot of Fig. 2. Also, this single triangular patch antenna has a gain of 5.9 dB as shown in Fig. 3 which shows also the three-dimensional radiation pattern of the single triangular patch antenna.

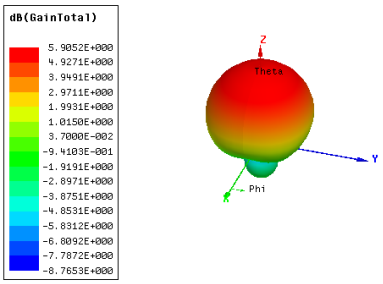

Fig. 3: 3D Radiation pattern of single patch antenna.

B. Two-Element Triangular Antenna Array

Fig. 4 shows the configuration of a two-element triangular patch antenna array. The impedance of the input transmission line feeder is 50 Ω with the same length and width of 1.15 mm and 0.25 mm respectively; this line is split into two 75 Ω lines with widths, W_{75}, 0.09 mm. The performance is found to be at its best when the spacing between the two elements is a half wavelength. After a parametric study on the different parameters of this array shown in Fig. 4, the values chosen are presented in table II.

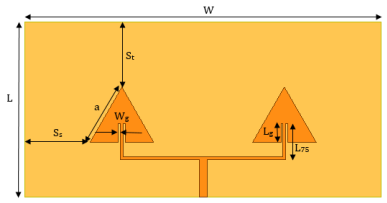

Fig. 4: Two-element antenna array geometry.

TABLE II: Two-element antenna array dimensions.

Parameters	Values (in mm)
L	5.38
W	10.96
a	1.959
S_t	2
S_s	2
W_g	0.06
L_g	0.58
L_{75}	1.02

It is worth to mention that the side length of the triangular patch is slightly different from the single element antenna and that is essential in order to have perfect matching at 30 GHz. Obviously, as shown in Fig. 5, this design resonates at approximately 30 GHz with a different value of reflection coefficient than the one obtained for the single elements. Fig. 6 shows the three dimensional radiation pattern of the two element antenna array. Note that the gain obtained is 8.57 dB, hence the gain increased by 45% by creating a two element array.

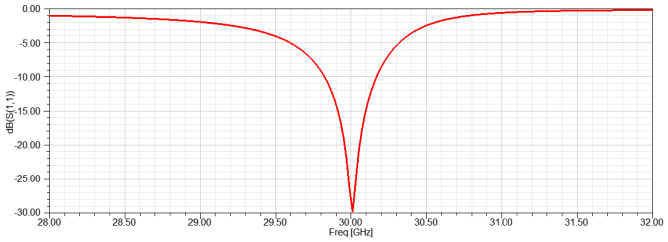

Fig. 5: S_{11} plot for the two-element antenna array.

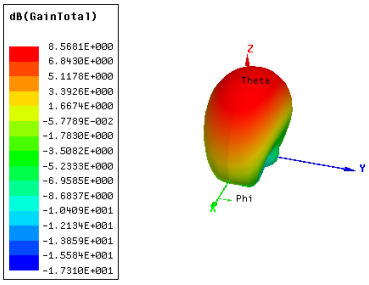

Fig. 6: 3D Radiation pattern for the two-element antenna array.

C. Three-Element Triangular Antenna Array

In order to further enhance the gain of the antenna, a third triangular patch is added to the array. Fig. 7 shows the three element antenna array and its dimensions are given in table III. The spacing between the elements placed horizontally is equal to half-wavelength however the third element is placed above the two by a distance of a quarter wavelength.

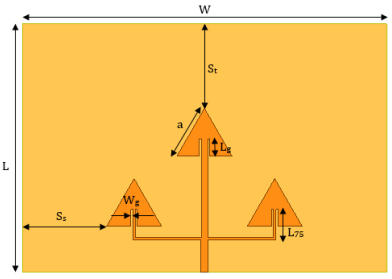

Fig. 7: Three-element antenna array geometry.

TABLE III: Three-element antenna array dimensions.

Parameters	Values (in mm)
L	8.83
W	12.95
a	1.95
S_t	3
S_s	3
W_g	0.07
L_g	0.6
L_{75}	1

The 50 Ω transmission feed line is split into three: two 75 Ω transmission lines that feed the two horizontally placed triangular elements and a third transmission line that has a value of approximately 50 Ω to feed the upper triangular patch. A good matching at a frequency around 30 GHz is achieved as shown in Fig. 8. This configuration turned out to have the best gain of 9.26 dB as shown in Fig. 9 representing the three dimensional plot of the radiation pattern for the array of three elements. Fig. 9 shows that the three element antenna array is the most directive antenna which validates the use of antenna arrays for directive millimeter wave propagation.

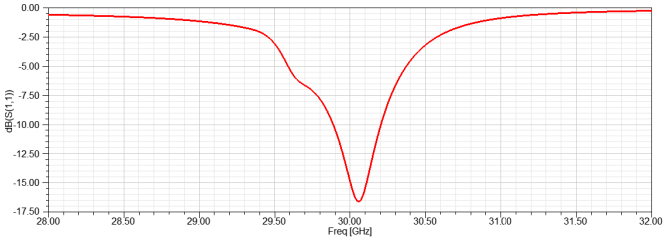

Fig. 8: S_{11} plot for the three-element antenna array.

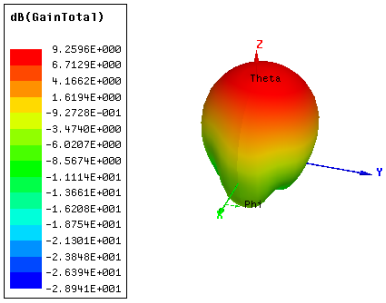

Fig. 9: 3D Radiation pattern for the three-element antenna array.

D. Fractal Design of Nine-Element Triangular Antenna Array

B. Mandelbrot proposed, in [21], the fractal theory which states that, in contrast with the Euclidean space, the space can have a fractional dimension based on the repetition of a certain shape. The authors of [22] proposed that a fractal geometry has a space-filling property which will result in designing miniature classic antenna elements. In this paper, the fractal design is generated by repeating the three-element triangular antenna array, three times; the three three-element antenna arrays are placed in a triangular shape also. Fig. 10 presents the geometry of the biggest antenna array of nine elements, designed using the previous three-element antenna array by the fractal design procedure. The dimensions of this antenna are presented in table IV.

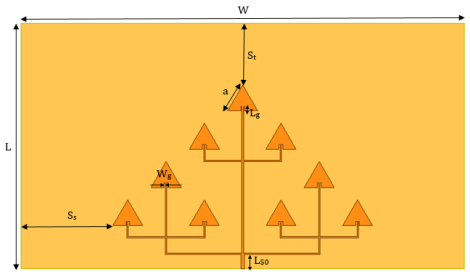

Fig. 10: Fractal nine-element antenna array geometry.

TABLE IV: Fractal nine-element antenna array dimensions.

Parameters	Values (in mm)
L	16
W	28.96
a	1.96
S_t	4
S_s	6
W_g	0.08
L_g	0.3
L_{75}	0.92

In this design, the feeding network is formed of the 50 Ω transmission line feeder split equally into three 75 Ω transmission lines which are, in turn, split into three 75 Ω transmission lines also. The side length of the triangular patched regained its size of 1.96 mm. A parametric study was done on several design parameters such as the side length of the triangle, the length and width of the inset feed, the spacing between the radiating patch and the edges of the substrate and the length and width of the transmission lines. Also, a parametric study was done on the spacing between the three-element triangular antenna array. Each array presents an element of the fractal design; the spacing between the horizontally placed elements is a wavelength which makes it a half-wavelength between each single triangular patch. The spacing between the two lower arrays and the one placed above them is also a half-wavelength. Fig. 11, the S_{11} plot, shows a good matching condition at 30 GHz and Fig. 12, the 3D plot of the radiation pattern, represents a gain of 12.51 dB and the radiation pattern is becoming more and more directive.

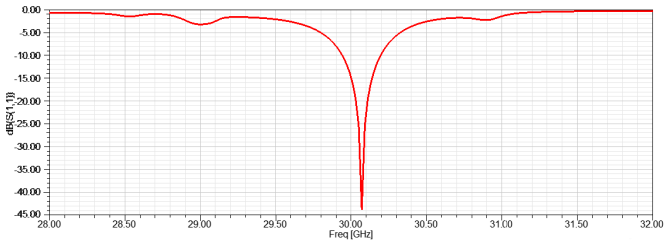

Fig. 11: S_{11} plot for the fractal nine-element antenna array.

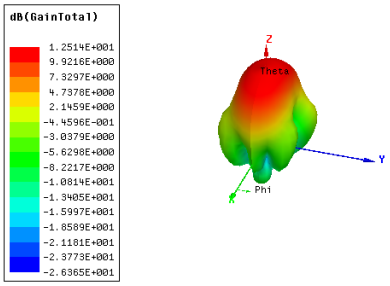

Fig. 12: 3D Radiation pattern for the fractal nine-element antenna array.

E. Nine-Element Triangular Antenna Array with Triangle-Shaped Ground Plane

In the same previous design of nine elements with minor modifications, the ground plane is cut into a triangular shape and the new antenna array is shown in Fig. 13 with all its dimensions in table V. The gap of the inset feed is removed and the dimensions are rounded to reduce the complexity of the antenna fabrication process. All transmission lines of this design are taken to be 50 Ω. Its reflection coefficient plot shown in Fig. 14 presents good matching conditions at around 30 GHz and multiple resonances appear at other frequencies. Its gain also increased to 12.5 dB as depicted in Fig. 15. The spacing between all the elements, the spacing from the edges and the feeding network design are kept unchanged.

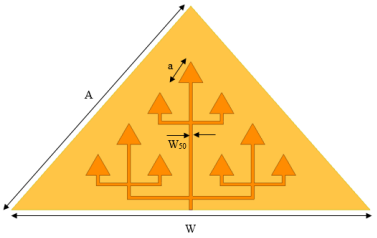

Fig. 13: Geomety of fractal nine-element antenna array withtriangular-shaped ground plane.

TABLE V: Dimensions of the fractal nine-element antenna array with triangular-shaped ground plane.

Parameters	Values (in mm)
A	21.96
W	29
a	1.96

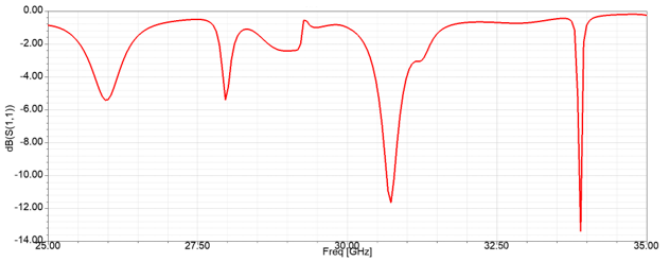

Fig. 14: S_{11} plot for the fractal nine-element antenna array with triangular-shaped ground plane.

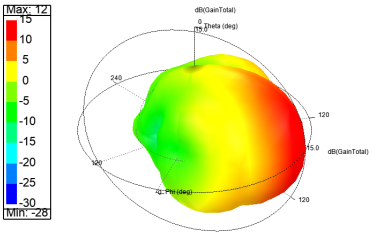

Fig. 15: 3D Radiation pattern for the fractal nine-element antenna array with triangular-shaped ground plane.

III. Fabricated Antenna and Measurements

Due to the fact that these antennas are very expensive to fabricate, the authors of this paper decided to fabricate only the triangular shaped antenna presented in the last part of the previous section. The antenna chosen to be fabricated is simulated again using CST Studio, Fig. 16, to get more accurate results while taking into account the effect the SMA connector, used to measure it, on its reflection coefficient and gain. The antenna fabricated is then measured to prove the simulated results.

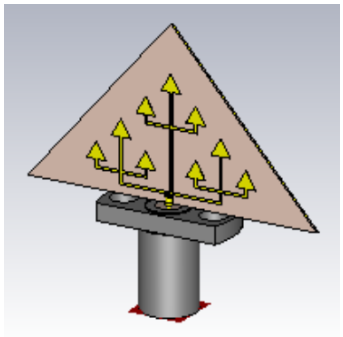

Fig. 16: Antenna Simulated on CST Studio.

The antenna fabricated is presented in Fig. 17. The simulated and the measured S_{11} are presented on the same plot in Fig. 18 that shows that resonance frequencies experienced shifts to slightly higher frequencies. Measured S_{11} presented better matching at resonant frequencies which is expected at high millimeter frequencies. As for the gain, Fig. 19a presents the gain obtained by simulation on CST; whereas Fig. 19b presents the measured gain of the antenna fabricated which

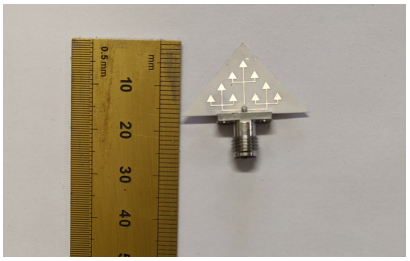

Fig. 17: Fabricated Antenna.

show that the measured design achieves a gain ranging from 6 to 10 GHz in the interval [32 - 34] GHz.

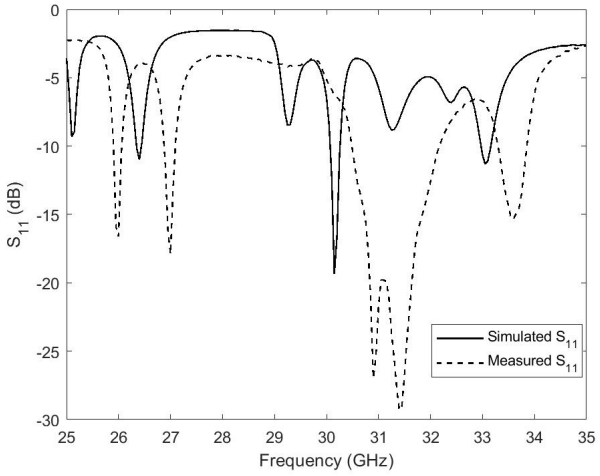

Fig. 18: Overlapped Simulated and Measured S_{11}.

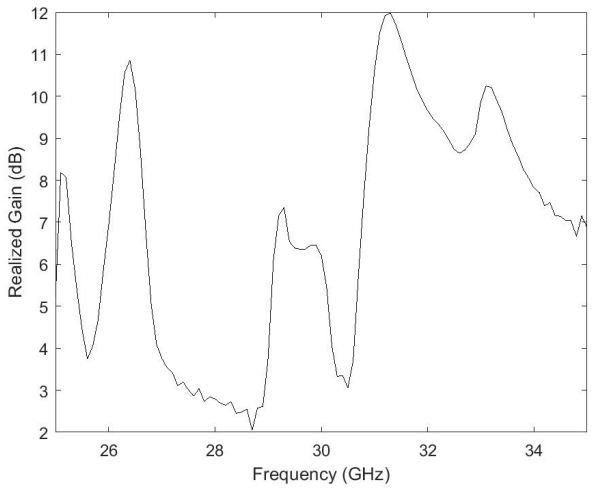

(a) CST Simulated Gain.

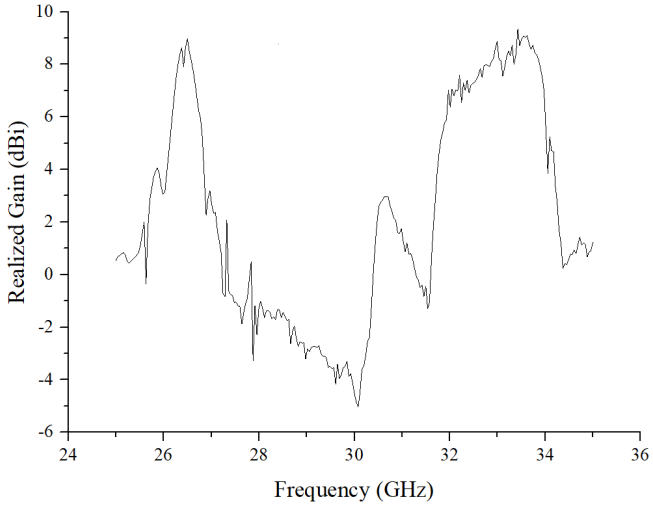

(b) Measured Gain.

Fig. 19: Triangular Antenna Gain.

IV. Three-dimensional antenna array designs

A third dimension is added to the design because additional gain is required but the occupied space is minimal, [23], consequently, a wider coverage is achieved. Multiple configurations could be done by placing several planar antenna arrays in proximity to each other with a convenient spacing between the arrays chosen after a parametric study to achieve the best gain possible with a trade-off between the gain and the size of the antenna.

In the following three-dimensional designs, all the planar antenna arrays exhibit a small shift in their resonance frequency; however, a very well matching condition at 30 GHz is achieved in all cases. The following three-dimensional designs are presented in descending order, from highest to lowest gain.

A. Design 1: Three triangular antenna arrays

This antenna shown in Fig. 20 has a gain of 16.52 dB, it consists of three planar triangular antenna arrays of the design shown in Fig. 13. The three antenna arrays are placed in the same xy-plane all facing the positive z-plane with a spacing of 2 mm between them. This design has three input points each coming from the 50 Ω input impedance.

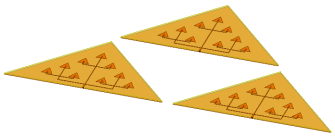

Fig. 20: Three triangular antenna arrays

B. Design 2: C-Curve

The antenna with a gain of 14.5 dB is shown in Fig. 21. It consists of three planar antennas of the design shown in Fig. 10, linearly placed in the same xy-plane all facing the

positive z-plane in a shape of a letter ”C” but with widely-opened extremities. The antenna arrays placed at the edges are tilted by 10° from the positive to the negative z-plane with a spacing of 5 mm between each two planar antennas. This design has three input points from the 50 Ω input impedances of the three planar antenna arrays.

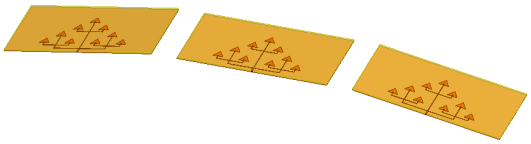

Fig. 21: C-Curve

C. Design 3: 3D Triangle

The antenna is shown in Fig. 22, it has a gain of 10.33 dB, it consists of three planar antennas of the design shown in Fig. 10. It resulted from the previous antenna, Fig. 21, however the tilt is 120° instead of 10°, to form a triangle. The three antenna arrays are placed like a triangle with a spacing of 2 mm between them. This design has three input points each coming from the 50 Ω input impedance.

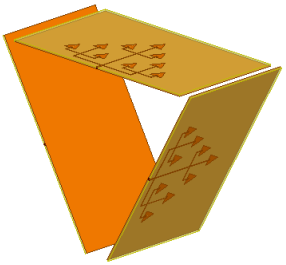

Fig. 22: 3D Triangle

D. Design 4: Three-faces pyramid

The antenna in Fig. 23, has a gain of 9.8 dB. Three planar triangular antenna arrays of the design shown in Fig. 13 placed like a pyramid with a tilting of 45° of each antenna array from the positive to the negative z-plane and with a spacing of 5 mm between each two arrays as depicted in Fig. 23. There are three input points coming from the 50 Ω input impedance of each antenna array.

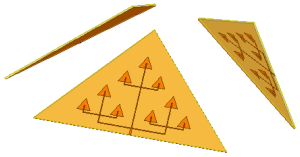

Fig. 23: Three-faces pyramid

E. Design 5: Four-faces pyramid

The antenna in Fig. 24 has a gain of 9.41 dB however it is formed of four planar triangular antenna arrays of the design shown in Fig. 13 placed like a four-faces pyramid. Similar to the antenna in Fig. 23, each antenna array is tilted by 45° from the positive to the negative z-plane and with a spacing of 5 mm between each two arrays as depicted in Fig. 24. There are four input points coming from the 50 Ω input impedance of each antenna array.

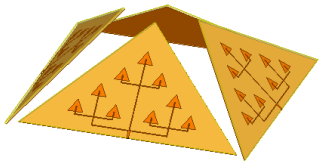

Fig. 24: Four-faces pyramid

F. Design 6: Right-standing three-faces pyramid/Crown

The same antenna is shown in both parts of Fig. 25 and it has a gain of 8.41 dB. It consists of three planar triangular antenna arrays of the design shown in Fig. 13. The three antenna arrays are placed like a crown with their bases forming an equilateral triangle and a spacing of 2 mm between them. This design has three input points each coming from the 50 Ω input impedance.

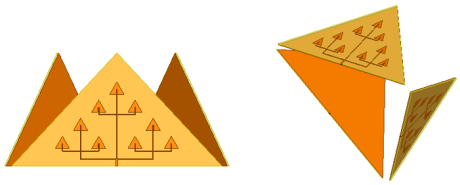

Fig. 25: Right-standing three-faces pyramid/Crown

G. Design 7: Cube

The antenna shown in Fig. 26 has a gain of 8.28 dB, it consists of four planar antennas of the design shown in Fig. 10. The four antenna arrays are placed like a cube with no spacing between them. This design has four input points each coming from the 50 Ω input impedance.

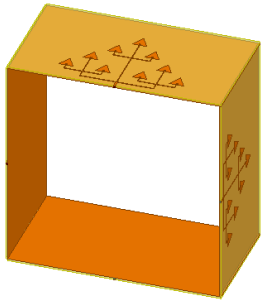

Fig. 26: Cube

After listing all the 3D designs, it could be seen that some antennas have lower gains than others, however, they present wider signal coverage. Fig. 27 shows the radiation pattern of some of three antennas (1, 6 and 7). Design 1 is radiating in only one direction with the highest gain of 16.52 dB, whereas design 6 is radiating in three directions with a lower gain of 8.41 dB and finally, design 7 is radiating in four directions with the lowest gain of 8.28 dB. Even though gain is decreasing, the 3D radiation pattern plots show that more areas in different directions could be covered using these designs. Therefore, an acceptable trade off between the gain and the covered regions should be made.

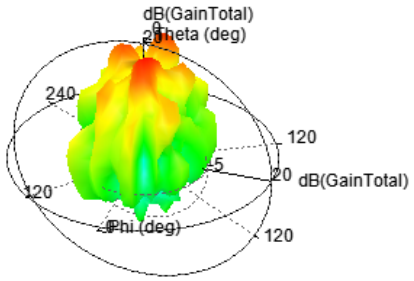

(a) Design 1.

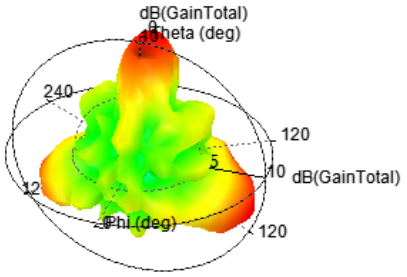

(b) Design 6.

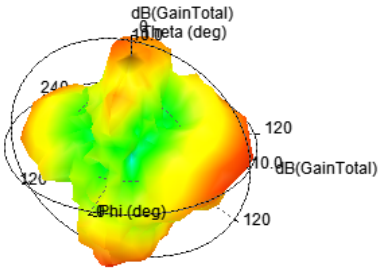

(c) Design 7.

Fig. 27: 3D Radiation Patterns of some of the 3D Designs.

V. Further Potential Applications

Recent studies in cancer detection are proposing imaging systems with a working frequency centered at 30 GHz, [24]. Cancer detection antenna systems, rely generally on the dielectric contrast between normal and infected tissues. Most of these systems operate on low frequencies which result in low resolution images and, therefore, preventing early detection. Using higher millimeter wave frequencies overpasses this issue while sacrificing the strength of the signal inside the breast tissues. Paper [25] proposes the use of beamforming algorithms to get an optimal image at an operational frequency of 30 GHz. High millimeter wave frequencies, [26], allow high resolution performances and other advantages of millimeter wave cancer detection systems are smaller size, higher comfortability and risk free since they retain tolerable penetration in human tissues. The detection process is based on the fact that a fraction of the radiated power, would be reflected back because of the discontinuity in the dielectric properties between the tissues.

VI. Conclusion

Multiple two-dimensional and multi-faceted three-dimensional printed antenna designs based on fractal-triangle shape are presented in this paper. One antenna prototype is fabricated and the results of the measured S11 and gain consistently match the simulated results, with a maximum 1 GHz shift. This antenna, resonating at multiple frequencies 26 GHz, 27 GHz, [30.5 - 32] GHz, 34 GHz and having a sufficient gain attaining 10 dB at around 26 GHz and 33 GHz, could be a good candidate for use at millimeter waves and 5G since it presents good performance in terms of reflection coefficient and high gain. All the antennas presented in this paper in addition to the one fabricated, could be used embedded in handheld devices thanks to their light-weight and small size.

References

[1] M. R. Bhalla and A. V. Bhalla, "Generations of mobile wireless technology: A survey," *International Journal of Computer Applications*, vol. 5, pp. 26–32, Aug. 2010.

[2] A. Nordrum, K. Clark, and I. S. Staff, "Everything you need to know about 5g," Jan. 2017.

[3] N. Lahoria, S. B. Rana, and N. Kumar, "5g future communication: Requirements and challenges," in *47 Mid-Term Symposium on Modern Information and Communication Technologies for Digital India*, Apr. 2016.

[4] A. Sebak, "High gain millimeter wave antennas for 5g wireless and security imaging systems," in *33rd National Radio Science Conference*, Feb. 2016.

[5] S. Chen and A. Zhao, "Ltcc based dual polarized magnetoelectric dipole antenna for 5g millimeter wave application," in *13th European Conference on Antennas and Propagation*, Apr. 2019.

[6] E. Yaacoub, M. Husseini, and H. Ghaziri, "An overview of research topics and challenges for 5g massive mimo antennas," in *IEEE Middle East Conference on Antennas and Propagation*, Sept. 2016.

[7] A. M. Jajere, "Millimeter wave patch antenna design - antenna for future 5g applications," *International Journal of Engineering Research & Technology*, vol. 6, pp. 289–291, Feb. 2017.

[8] H. Aliakbari, A. Abdipour, A. Costanzo, D. Masotti, R. Mirzavand, and P. Mousavi, "Ann based design of a versatile millimeter wave slotted patch antenna configuration for 5g scenarios," *IET Microwaves, Antennas & Propagation*, vol. 11, pp. 1288–1295, June 2017.

[9] Z. Ren, A. Zhao, and S. Wu, "Dual band mimo antenna system for 5g mobile terminals," in *13th European Conference on Antennas and Propagation*, Apr. 2019.

[10] Y. Liu, Y. Lu, Y. Zhang, and S.-x. Gong, "Mimo antenna array for 5g smartphone applications," in *13th European Conference on Antennas and Propagation*, Apr. 2019.

[11] Y. S. H. Khraisat and M. M. Olaimat, "Comparison between rectangular and triangular patch antennas array," in *19th International Conference on Telecommunications*, Apr. 2012.

[12] V. R. Ekke and P. L. Zade, "Design and implementation of t-junction triangular microstrip patch antenna array for wireless applications," *International Journal of Engineering and Technology*, vol. 8, pp. 2105–2114, Nov. 2016.

[13] N. Ojaroudiparchin, M. Shen, and G. F. Pedersen, "Design of vivaldi antenna array with end fire beam stearing function for 5g mobile terminals," in *23rd Telecommunications Forum*, Nov. 2015.

[14] R. Parolari, M. Gallo, A. P. Filisan, D. Zamberlan, V. Franchina, M. A., and P. Nepa, "A novel 3d antenna for lte mimo systems," in *International Conference of Electrical and Electronic Technologies for Automotive*, June 2017.

[15] P. Fernandez-Martinez, S. Martin-Anton, and D. Segovia-Vargas, "Design of a wideband vivaldi antenna for 5g base stations," in *IEEE International Symposium on Antennas and Propagation and USNC-URSI Radio Science Meeting*, July 2019.

[16] C.-Z. Han, G.-L. Huang, T. Yuan, and C.-Y.-D. Sim, "A dual band millimeter wave antenna for 5g mobile applications," in *IEEE International Symposium on Antennas and Propagation and USNC-URSI Radio Science Meeting*, July 2019.

[17] T. H. Choi, S. S. Kim, Y. J. Yoon, and H. Kim, "Wide band slot antenna on metal bezel for covering 28/39 ghz in 5g communication system," in *IEEE International Symposium on Antennas and Propagation and USNC-URSI Radio Science Meeting*, July 2019.

[18] T. Varum and J. Matos, "Compact slot antenna array for 5g communications," in *IEEE International Symposium on Antennas and Propagation and USNC-URSI Radio Science Meeting*, July 2019.

[19] P. Sravani and M. Rao, "Design of 3d antennas for 24 ghz ism band applications," in *28th International Conference on VLSI Design*, Jan. 2015.

[20] A. El-Bacha and R. Sarkis, "Design of tilted taper slot antenna for 5g base station antenna circular array," in *IEEE Middle East Conference on Antennas and Propagation*, Sept. 2016.

[21] Y.-H. Yu and C.-P. Ji, "Research of fractal technology in the design of multi frequency antenna," in *China-Japan Joint Microwave Conference*, Apr. 2011.

[22] M. A. Madi, M. Al-Husseini, A. H. Ramadan, K. Y. Kabalan, and A. El-Hajj, "A reconfigurable cedar shaped microstrip antenna for wireless applications," *Progress in Electromagnetics Research*, vol. 25, pp. 209–221, 2012.

[23] D. Huebner, "Directivity characteristics of 3 dimensional antennas," in *Antennas and Propagation Society International Symposium*, June 1985.

[24] S. Di Meo, P. F. Espin-Lopez, A. Martellosio, M. Pasian, M. Bozzi, L. Perregrini, A. Mazzanti, F. Svelto, P. E. Summers, R. G., P. L., and M. Bellomi, "Dielectric properties of breast tissues: Experimental results up to 50 ghz," in *12th European Conference on Antennas and Propagation*, Apr. 2018.

[25] S. Di Meo, G. Matrone, M. Pasian, L. Bozzi, M. Perregrini, G. Magenes, M. A., S. F., P. E. Summers, R. G., P. L., and M. Bellomi, "High resolution millimeter wave imaging techniques and systems for breast cancer detection," in *IEEE MTT-S International Microwave Workshop Series on Advanced Materials and Processes for RF and THz Applications*, Sept. 2017.

[26] S. Moscato, G. Matrone, M. Pasian, A. Mazzanti, M. Bozzi, L. Perregrini, F. Svelto, G. Magenes, P. Arcioni, and P. Summers, "A mm wave 2d ultra wide band imaging radar for breast cancer detection," *International Journal of Antennas and Propagation*, pp. 1–8, 2013.